Nuclear Magnetic Resonance Investigations of Configurational Non-rigidity in Dinuclear Platinum(IV) Complexes. Part 5.† Intramolecular Rearrangements in the Dinuclear Platinum(IV) Complexes of 1,3,5,7-Tetrathiocane. *X*-Ray Crystal Structure of $[(PtClMe_3)_2(SCH_2SCH_2SCH_2SCH_2)]$ ‡

Edward W. Abel, Gary D. King, Keith G. Orrell,* and Vladimir Šik
Department of Chemistry, University of Exeter, Exeter EX4 4QD
T. Stanley Cameron and Klaus Jochem
Department of Chemistry, Dalhousie University, Halifax B3 4J3, Canada

The complexes $[(PtXMe_3)_2(SCH_2SCH_2SCH_2SCH_2)]$ (X = Cl, Br, or I) have been prepared by direct reaction of 1,3,5,7-tetrathiocane with the appropriate halogenotrimethylplatinum(IV) tetramer, $[(PtXMe_3)_4]$ (X = Cl, Br, or I). The *X*-ray crystal diffraction structure of $[(PtClMe_3)_2(SCH_2SCH_2SCH_2SCH_2)]$ shows the dimeric platinum moiety to be 1,3-co-ordinated to the ligand which has a chair–boat conformation. Low-temperature ^1H n.m.r. spectroscopy confirms such a structure to be retained in solution for all three complexes. Lineshape changes observed in variable-temperature ^1H n.m.r. investigations are consistent with the complexes undergoing metal-pivot and platinum–methyl intramolecular rearrangements. Alternative mechanisms are discussed for both processes. It is concluded that the former comprises a series of 90° 1,5-metal pivots, and the latter, 120° rotations of methyl groups on the commuting Pt atom. Full bandshape analyses have been undertaken for both motions. Evidence is presented in support of the two fluxions being different manifestations of one transition state rather than independent rearrangements.

Hydrogen-1 n.m.r. investigations have revealed that complexes of the stoicheiometry $[(PtXMe_3)_2L]$ (X = Cl, Br, or I), where L is a linear bidentate ligand, undergo a remarkable variety of intramolecular conformational and configurational rearrangements.[1]

Recently, we [2] carried out a study on analogous complexes in which L was a six-membered heterocyclic system. A detailed examination of the complexes of 1,3,5-trithiane $[(PtXMe_3)_2(SCH_2SCH_2SCH_2)]$ (X = Cl or Br), showed the dimeric halogen-bridged platinum(IV) moiety to commute between co-ordinated and unco-ordinated sulphur atom pairs *via* a series of intramolecular 60° 1,3-pivots about individual S–Pt bonds.

In a closely related field of study, the magnitude of $\Delta G^{\ddagger}$ (298.15 K) for 1,3-metal shifts in the complexes $[M(CO)_5\{SCH(R)SCH(R)SCH(R)\}]$ (M = Cr or W, R = H or Me) was observed to be dependent upon the skeletal flexibility of the ligand system.[3,4]

As a logical extension to the above work, it was decided to investigate the effects (if any) of increased ligand flexibility on the pivoting motion observed previously in dimeric Pt^{IV} complexes of 1,3,5-trithiane. Frank *et al.*[5] have shown ring reversal in 1,3,5,7-tetrathiocane to be rapid even at −170 °C. This demonstrates a considerable increase in skeletal flexibility in comparison with 1,3,5-trithiane which has a ring-reversal coalescence temperature of −33 °C.[6]

This work, therefore is concerned with the synthesis, characterisation, and dynamic n.m.r. spectroscopic analysis of stereochemical non-rigidity in the hitherto unknown dimeric platinum(IV) complexes of 1,3,5,7-tetrathiocane, $[(PtXMe_3)_2(SCH_2SCH_2SCH_2SCH_2)]$ (X = Cl, Br, or I).

Experimental

Materials.—The following starting materials were prepared and purified using literature procedures: 1,3,5,7-tetrathiocane,[7,8] m.p. 48—49 °C (lit.[7] 48.5 °C); trimethylplatinum(IV) iodide [9] was converted to trimethylplatinum(IV) sulphate [10] and the other trimethylplatinum(IV) halides obtained by reaction of the latter with the appropriate potassium halide.[11]

Since the preparations of the complexes were very similar a representative method for the chloride complex is given. Analytical data are in Table 1.

Di-μ-chloro-μ-1,3,5,7-tetrathiocane-bis[trimethylplatinum(IV)].—A solution of trimethylplatinum(IV) chloride (151 mg, 0.14 mmol) and 1,3,5,7-tetrathiocane (57 mg, 0.31 mmol)‡ in AnalaR chloroform (15 cm^3) was refluxed routinely under nitrogen for 6 h, then stirred for an additional 2 h at room temperature. All solvent was removed under reduced pressure, and the white residue washed with light petroleum (b.p. 40—60 °C). Recrystallisation of the solid from chloroform–light petroleum (b.p. 40—60 °C) gave the product as shining white crystals (139 mg, 69%).

Crystal Data.—$C_{10}H_{26}Cl_2Pt_2S_4$, $M = 735.53$, triclinic, $a = 10.344(2)$, $b = 11.915(4)$, $c = 12.758(3)$ Å, $\alpha = 132.42(2)$, $\beta = 91.16(2)$, $\gamma = 113.50(2)°$, space group $P\bar{1}$, $Z = 2$, $D_c = 2.539$ g cm^{-3}, Mo-K_α radiation ($\lambda = 0.710\,69$ Å).

2 664 Independent observable reflections were collected on a four-circle diffractometer, of which 2 017 had $I > \sigma(I)$. The structure was solved by tangent and Fourier methods and

† Part 4 is ref. 32.

‡ Di-μ-chloro-μ-(1,3,5,7-tetrathiocane-S^1,S^3)-bis[trimethylplatinum(IV)].

Supplementary data available (No. SUP 23981, 27 pp.): structure factors, thermal parameters. See Instructions for Authors, *J. Chem. Soc., Dalton Trans.*, 1984, Issue 1, pp. xvii—xix.

‡ Molar quantities are based on the tetrameric unit $[(PtClMe_3)_4]$.

Table 1. Characterisation of the dinuclear platinum(IV) complexes of 1,3,5,7-tetrathiocane

Complex	Yield (%)	M.p. [a] (°C)	Microanalysis [b] (%) C	H
$[(PtClMe_3)_2(SCH_2SCH_2SCH_2SCH_2)]$	69	216	16.1 (16.3)	3.60 (3.55)
$[(PtBrMe_3)_2(SCH_2SCH_2SCH_2SCH_2)]$	57	188	14.5 (14.5)	3.00 (3.20)
$[(PtIMe_3)_2(SCH_2SCH_2SCH_2SCH_2)]$	67	165	14.1 (13.1)	3.15 (2.85)

[a] With decomposition. [b] Calculated values are in parentheses.

refined by least squares. The conventional R value was 0.04, with isotropic thermal parameters on the hydrogen atoms and anisotropic parameters on all other atoms. Final atomic co-ordinates are given in Table 2.

N.M.R. Studies.—All ^1H spectra of the complexes were recorded on a JEOL PS/PFT-100 spectrometer using $CDCl_3$ as solvent. A JES-VT-3 variable-temperature unit was used to control the probe temperature. The latter was measured to an accuracy of within 1 °C using a Comark digital thermometer (Type 5000) attached to a Cu/Cu–Ni thermocouple adapted for use in the n.m.r. probe.

Bandshape analyses. These were carried out using modified versions [12] of the original DNMR3 program of Kleier and Binsch.[13] Computer simulated and variable-temperature experimental spectra were compared visually until the 'best fits' were obtained. Arrhenius and Eyring energy parameters were calculated in the usual way. The errors quoted for the Eyring free energies of activation ($\Delta G^{\ddagger}$) are calculated from the standard deviation term $|\sigma(\Delta H^{\ddagger}) - T\sigma(\Delta S^{\ddagger})|$ as described by Binsch and Kessler.[14]

Results

Properties of the Complexes.—The complexes $[(PtXMe_3)_2(SCH_2SCH_2SCH_2SCH_2)]$ were obtained as white (X = Cl and Br) or pale yellow (X = I), air stable, crystalline solids. They are involatile and decompose on heating without melting. Analytical data (Table 1) are consistent with the complexes containing a dimeric halogenotrimethylplatinum(IV) moiety.

A poor solubility in chloroform was observed, rapidly decreasing in the order I > Br > Cl.

Although the complexes are stable to aerial oxidation in solution, ^1H n.m.r. spectroscopy showed ligand dissociation–recombination to occur above ambient temperature: *ca.* 28 (X = I), 48 (Br), or 60 °C (Cl).

X-Ray Crystal Structure of Di-μ-chloro-μ-1,3,5,7-tetrathiocane-bis[trimethylplatinum(IV)].—The *X*-ray data of $[(PtClMe_3)_2(SCH_2SCH_2SCH_2SCH_2)]$ produced the structure shown in Figure 1.[15] Selected bond length and angle data are given in Table 3.

In general, the dinuclear moiety of the molecule has bond lengths identical with those in $[(PtClMe_3)_4]$.[16,17] The configuration about each Pt atom is approximately octahedral, with the interbond angles in the ranges 177.3—178.9 and 86.2—93.5°. The Pt · · · Pt contact is 3.633(1) Å which compares with 3.621(1) Å for the weak Pt · · · Pt interaction in di-μ-chloro-μ-1,3,5-trithiane-bis[trimethylplatinum(IV)].[18,19] Furthermore, the above value contrasts with 3.418(1) Å for the moderate Pt · · · Pt interaction in $[Pt_2Cl_6]^{2-}$ (ref. 20) and 2.652(2) Å in bis[μ-bis(diphenylphosphino)methane]-bis-[chloroplatinum(I)] where there is a strong Pt–Pt bond.[21]

Table 2. Atomic co-ordinates

Atom	*X/a*	*Y/b*	*Z/c*
Pt(1)	0.8921	0.8460	1.1433
Pt(2)	0.7028	0.4635	0.7168
S(1)	0.5717	0.6103	0.7423
C(1)	0.6634	0.8472	0.9239
H(11)	0.7601	0.9204	0.9177
H(12)	0.5778	0.8773	0.9236
S(2)	0.7416	0.9492	1.1170
C(2)	0.5699	0.8735	1.1462
H(21)	0.6080	0.9425	1.2651
H(22)	0.5091	0.7274	1.0649
S(3)	0.4355	0.9191	1.1165
C(3)	0.2685	0.6927	0.9405
H(31)	0.1685	0.7015	0.9410
H(32)	0.2543	0.6040	0.9483
S(4)	0.2697	0.5847	0.7537
C(4)	0.3875	0.5008	0.7364
H(41)	0.3221	0.3564	0.6259
H(42)	0.4098	0.5194	0.8318
Cl(1)	0.9545	0.7731	0.9244
Cl(2)	0.6598	0.5208	0.9373
Me(11)	1.0266	0.7723	1.1739
H(111)	0.9559	0.6272	1.0984
H(112)	1.0717	0.8483	1.2948
H(113)	1.1224	0.8028	1.1446
Me(12)	0.8376	0.9009	1.3210
H(121)	0.7322	0.7795	1.2720
H(122)	0.8200	1.0105	1.3821
H(123)	0.9320	0.9417	1.4023
Me(13)	1.0848	1.1110	1.3071
H(131)	1.0544	1.1967	1.3225
H(132)	1.1760	1.1150	1.2673
H(133)	1.1252	1.1606	1.4176
Me(21)	0.8098	0.3393	0.6901
H(211)	0.9323	0.4416	0.7689
H(212)	0.7962	0.2427	0.5704
H(213)	0.7574	0.2677	0.7167
Me(22)	0.5001	0.2097	0.5485
H(221)	0.4065	0.2214	0.5285
H(222)	0.4737	0.1491	0.5871
H(223)	0.5125	0.1241	0.4408
Me(23)	0.7472	0.4249	0.5424
H(231)	0.7025	0.4794	0.5220
H(232)	0.6911	0.2801	0.4358
H(233)	0.8715	0.4948	0.5775

The two Pt–S co-ordination bonds have a mean length of 2.475 Å which compares well with 2.465 Å for the analogous bonds in the aforementioned chloro-complex of 1,3,5-trithiane.[18,19]

The eight-membered ring of the 1,3,5,7-tetrathiocane ligand retains the boat–chair conformation previously identified [22] for the ligand in its unco-ordinated crystalline state. The eight S–C bond lengths are not significantly

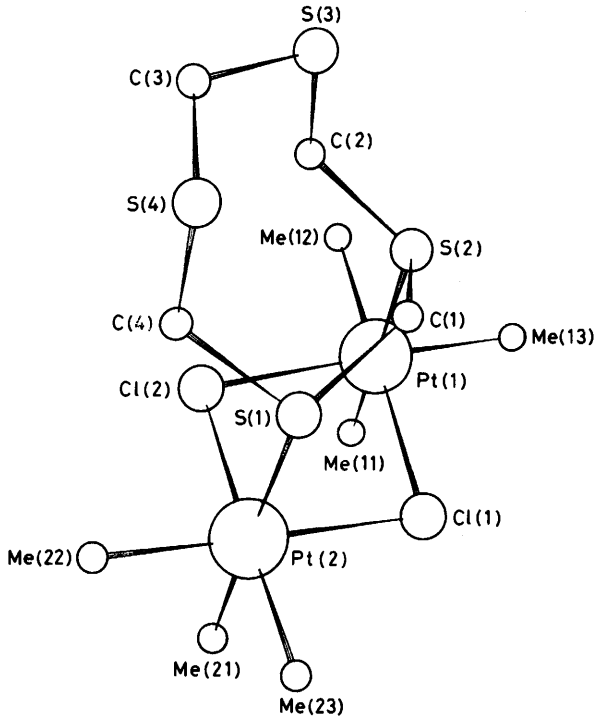

Figure 1. A PLUTO perspective view of the molecular structure of $[(PtClMe_3)_2(SCH_2SCH_2SCH_2SCH_2)]$ showing the numbering scheme used in Table 3

Table 3. Bond lengths (Å) and bond angles (°) in $[(PtClMe_3)_2(SCH_2SCH_2SCH_2SCH_2)]$

(*a*) Bond lengths

Pt(1)–S(2)	2.472(5)	Pt(2)–S(1)	2.478(5)
Pt(1)–Cl(1)	2.493(5)	Pt(2)–Cl(1)	2.506(5)
Pt(1)–Cl(2)	2.505(5)	Pt(2)–Cl(2)	2.507(5)
Pt(1)–Me(11)	2.068(28)	Pt(2)–Me(21)	2.043(24)
Pt(1)–Me(12)	2.057(26)	Pt(2)–Me(22)	2.038(21)
Pt(1)–Me(13)	2.054(25)	Pt(2)–Me(23)	2.049(26)
S–C (average)	1.800		

(*b*) Bond angles

S(2)–Pt(1)–Cl(1)	89.6(2)	S(1)–Pt(2)–Cl(1)	89.3(2)
S(2)–Pt(1)–Cl(2)	91.6(2)	S(1)–Pt(2)–Cl(2)	90.0(2)
S(2)–Pt(1)–Me(11)	177.3(8)	S(1)–Pt(2)–Me(21)	178.6(7)
Cl(1)–Pt(1)–Cl(2)	86.6(2)	Cl(1)–Pt(2)–Cl(2)	86.2(2)
Cl(1)–Pt(1)–Me(11)	90.8(8)	Cl(1)–Pt(2)–Me(21)	91.4(7)
Cl(1)–Pt(1)–Me(12)	178.9(7)	Cl(1)–Pt(2)–Me(22)	178.8(6)
Cl(2)–Pt(1)–Me(11)	91.1(8)	Cl(2)–Pt(2)–Me(21)	91.4(7)
Cl(2)–Pt(1)–Me(12)	92.4(7)	Cl(2)–Pt(2)–Me(22)	93.5(6)
Cl(2)–Pt(1)–Me(13)	178.3(7)	Cl(2)–Pt(2)–Me(23)	177.7(7)
Me(11)–Pt(1)–Me(12)	89(1)	Me(21)–Pt(2)–Me(22)	88(1)
Me(11)–Pt(1)–Me(13)	89(1)	Me(21)–Pt(2)–Me(23)	88(1)
Me(12)–Pt(1)–Me(13)	89(1)	Me(22)–Pt(2)–Me(23)	89(1)
Pt(1)–S(2)–C(1)	115.3(7)	Pt(2)–S(1)–C(1)	116.5(7)
Pt(1)–S(2)–C(2)	107.2(7)	Pt(2)–S(1)–C(4)	106.9(7)
Pt(1)–Cl(1)–Pt(2)	93.2(2)	S(1)–C(1)–S(2)	125(1)
Pt(1)–Cl(2)–Pt(2)	92.9(2)	S(2)–C(2)–S(3)	114(1)
		S(3)–C(3)–S(4)	119(1)
C–S–C (average)	103.5	S(4)–C(4)–S(1)	115(1)

different. These have a mean length of 1.800 Å in comparison with 1.817 Å in the free ligand.[22]

The non-bonding S · · · S contact of the bridging portion of the ring is 3.19(1) Å such that the two S atoms do not exactly span the Pt · · · Pt distance. This causes some distortion in the ring, the S(1)–C(1)–S(2) interbond angle being 125° in contrast to 114—119° for all the other S–C–S angles. The strain in the system is further relieved by a slight bending of the two Cl–Pt–Cl fragments, the angles between the normals to the planes being 10.5°. A similar distortion (29°) of the halogen bridge moiety has been observed in $[(PtBrMe_3)_2(MeSeSeMe)]$.[23]

Hydrogen-1 N.M.R. Studies.—The three complexes $[(PtXMe_3)_2(SCH_2SCH_2SCH_2SCH_2)]$ (X = Cl, Br, or I) showed similar spectral features. The complex with X = Br is taken as being typical.

Low-temperature 'static' spectra. The 100-MHz proton spectrum ($CDCl_3$, *ca.* −25 °C) showed two groups of well resolved signals (see Figure 2). Analysis of this 'static' spectrum shows it to be consistent with the complex having retained the solid-state structure described above.

The platinum–methyl region consists of three distinct signals R, S, and T (plus ^{195}Pt satellites) in a ratio of 1 : 1 : 1. These correspond to the three Pt–Me environments that exist in the proposed solution structure of the complex (Figure 3). The assignment of different methyl environments to particular spectral resonances is in line with previous arguments regarding closely related complexes.[2,24]

The ^1H n.m.r. data for the Pt–Me signals of all three complexes are collected in Table 4. The trends in $^2J(^{195}Pt–^1H)$ couplings reflect *trans* and *cis* halogen influences, as noted previously.[24,25]

The ligand-methylene region of the spectrum demonstrates a greater degree of complexity. As a consequence of deshielding influences and the introduction of chemical and magnetic anisotropy, four distinguishable methylene environments are observed (Figure 2) as opposed to one in uncoordinated tetrathiocane.[5] The assignment of individual resonances/multiplets to individual methylene environments (Figure 3) is made as follows.

By direct analogy with the dinuclear platinum(IV) complexes of 1,3,5-trithiane,[2] the bridging methylene group, AB, resonates at the highest frequency. Since the protons of this group are chemically and magnetically distinct, an AB-type quartet ($^2J_{gem} \simeq -15$ Hz) is not unexpected. The high-frequency component of the quartet, in accordance with proposals of Campaigne *et al.*,[26] is attributed to the pseudo-axial methylene proton, A. This assignment is further substantiated by this component comprising two overlapping 'quintets,' each possessing an intensity ratio of 1 : 7.8 : 17.5 : 7.8 : 1. This is consistent with A coupling equally to two Pt atoms.[27–29] Assuming the Karplus equation [30] to be applicable, a $^3J(^{195}Pt–^1H_A)$ value of *ca.* 13 Hz implies an H_A–C/S–Pt dihedral angle of either approximately 0 or 180°. In Figure 3, this dihedral angle is 180 and 60° for an axial and equatorial group respectively. Thus, the methylene proton A is shown in the correct environment, axial to the ligand ring.

The resonances for the remaining methylene groups, CD and EF, are immediately distinguishable by integration, being 2 : 1 respectively. Their relative positioning and extent of Pt coupling are as anticipated.

Spectral data for the ligand-methylene signals of all three complexes are collected in Table 5.

Dynamic spectra. Upon warming $CDCl_3$ solutions of the complexes above −25 °C lineshape changes were concurrently observed in both of the above spectral regions. These are described separately below. Although ligand dissociation–

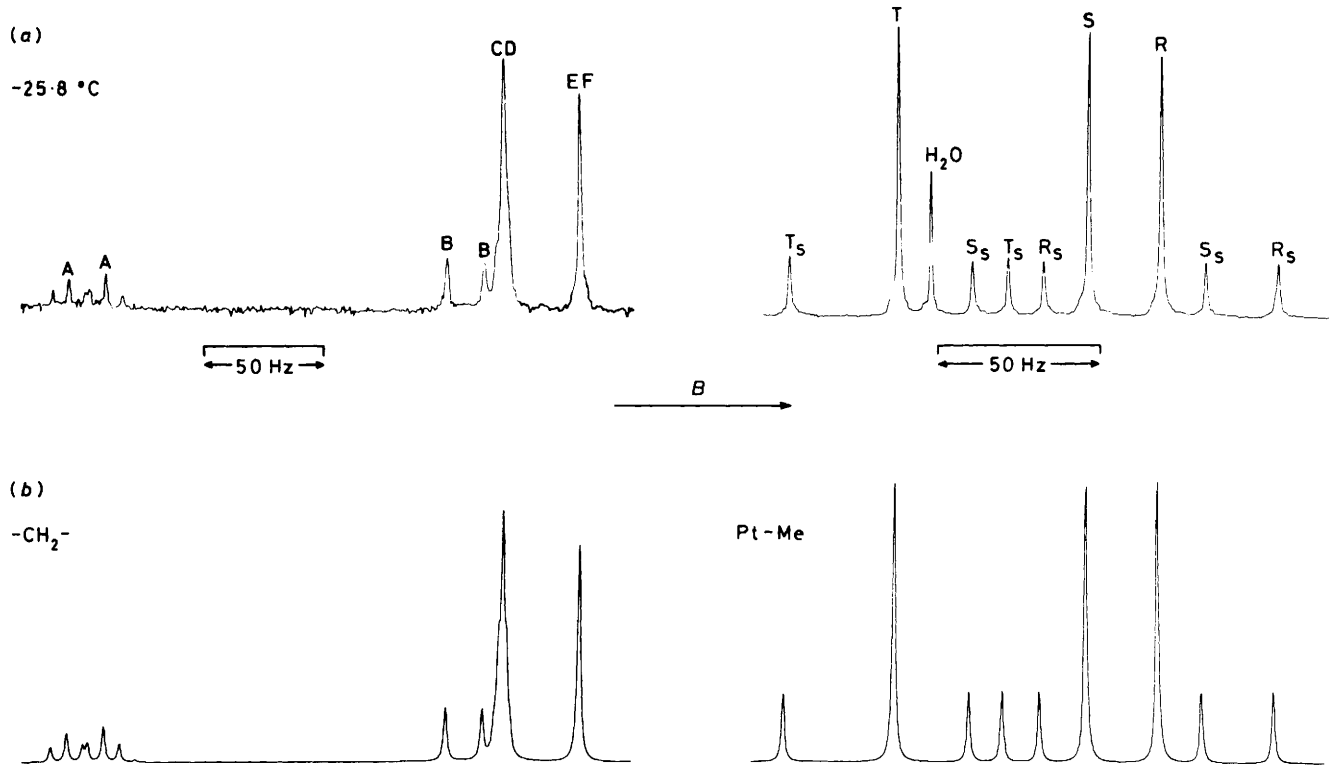

Figure 2. (*a*) Experimental and (*b*) computer-simulated ^1H n.m.r. spectra (100 MHz) of the Pt–methyl and ligand-methylene regions of $[(PtBrMe_3)_2(SCH_2SCH_2SCH_2SCH_2)]$. Band assignments are in accordance with Figure 3 (subscript s = ^{195}Pt satellite)

Table 4. Static platinum–methyl ^1H n.m.r. parameters [a] used in the lineshape analyses of methyl scrambling in the complexes $[(PtXMe_3)_2(SCH_2SCH_2SCH_2SCH_2)]$ (X = Cl, Br, or I)

X in the complex	θ/°C	T_2^* [b]/s	ν_R	ν_S	ν_T	$^2J(^{195}Pt-^1H_R)$	$^2J(^{195}Pt-^1H_S)$	$^2J(^{195}Pt-^1H_T)$
Cl	−16.4	0.180	86.91	110.83	166.25	77.15	76.90	71.05
Br	−25.8	0.286	96.19	119.62	182.62	76.66	76.17	71.77
I	−32.9	0.286	112.37	135.62	212.52	74.72	74.48	73.24

[a] In Hz unless otherwise specified. Recorded in $CDCl_3$ relative to $SiMe_4$. [b] $T_2^* = (\pi\Delta\nu_{\frac{1}{2}})^{-1}$, where $\Delta\nu_{\frac{1}{2}}$ is the linewidth (Hz) at half-height in the absence of exchange.

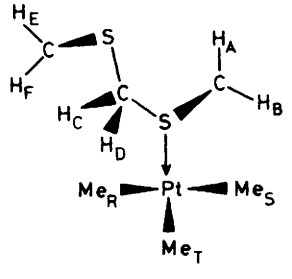

Figure 3. Solution structure of $[(PtBrMe_3)_2(SCH_2SCH_2SCH_2SCH_2)]$ as viewed directly along the Pt · · · Pt axis. The labelling of protons is in accordance with Figure 2

recombination was observed at temperatures beyond coalescence, sufficient predissociation spectra were obtained to allow full analyses of the intramolecular processes occurring.

Ligand-methylene region. With increased temperature, the signals of the four methylene environments were observed to broaden and coalesce together (see Figure 4). As in the Pt^{IV} complexes of 1,3,5-trithiane,[2] this averaging was thought to be a consequence of the dinuclear metal moiety commuting over all S atoms *via* a series of 60° 1,3-pivots about any one S–Pt bond. However, the 'additional' unco-ordinated atom of the tetrathiocane ligand might conceivably mean that the process proceeds *via* a six-co-ordinate *intermediary* species rather than a seven-co-ordinate *transition state*, see later. Spectral and steric considerations, discussed later, show this not to be so. The metal-pivot process, therefore, is analogous to that previously observed in the trithiane complexes. The energy barriers associated with this motion were assessed by simulation of spectral lineshape changes based on the simplified spin problem for the methylene protons shown in Scheme 1 (X = ^{195}Pt).

Experimental and computed spectra of the ligand-methylene protons in the iodo-complex are shown in Figure 4 (note that the signals for the bridging methylene proton A are not shown). The dissimilarity between the experimental and simulated spectra at 33.5 °C, the latter being calculated using a rate (of pivot) obtained by extrapolation of the appropriate Arrhenius plot, illustrates the effect of intermolecular ligand dissociation–recombination on lineshape.

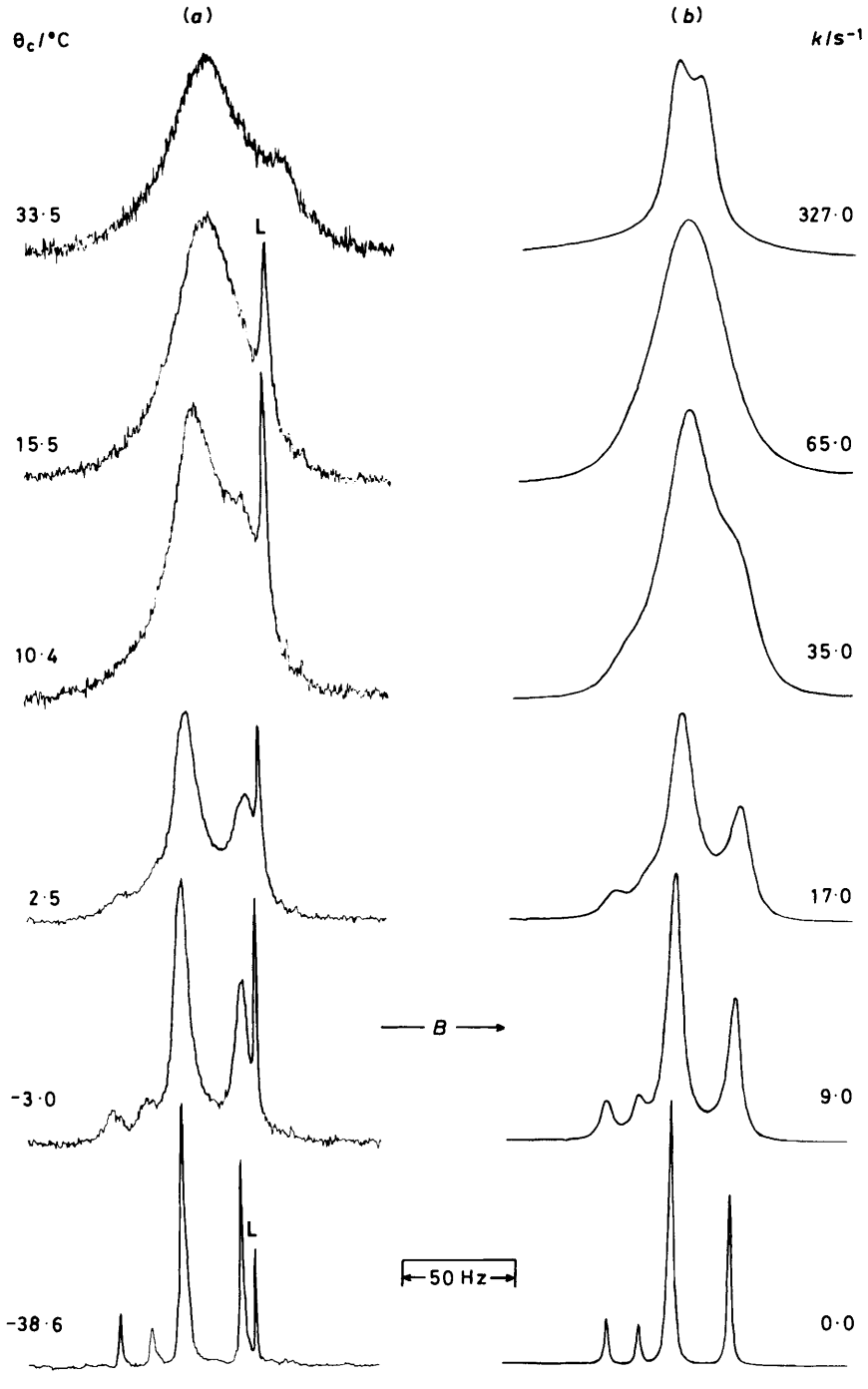

Figure 4. (*a*) Experimental and (*b*) computer-simulated spectra (ligand-methylene region) of $[(PtIMe_3)_2(SCH_2SCH_2SCH_2SCH_2)]$, demonstrating the effects of metal pivoting (L = free ligand)

The static parameters used in the above simulation are given in Table 5, and the activation parameters obtained, in Table 6. The Arrhenius plot for the pivot motion in the bromo-complex is shown in Figure 5.

Platinum–methyl scrambling. Concurrent with the onset of ligand pivoting, spectral changes were observed in the Pt–Me signals (see Figure 6) consistent with an averaging (scrambling [31]) of all Pt–Me environments. Examination of the variable-temperature spectra reveals the rate of exchange between equatorial environments to be greater than that between equatorial and axial. This is adequately interpreted by considering the effects of metal pivoting on the *trans* to halogen (*i.e.* equatorial) Me groups that are on the 'pseudo-stationary' Pt atom. Although it is assumed that these groups cannot scramble (see later), one pivot will interchange the two equatorial environments (see Figure 7). Since both sets of Me groups contribute equally to the n.m.r. spectral appearance this, therefore, explains the above observation.

Such effects were incorporated into the dynamic spin problem (Scheme 2; X = ^{195}Pt) used to calculate the activation parameters of the methyl-scrambling process (Table 6). The rate constant of equatorial–equatorial methyl exchange, k'',

Table 5. Static ligand-methylene ^1H n.m.r. parameters used in the lineshape analysis of 1,5-metal pivots in the complexes $[(PtXMe_3)_2(SCH_2SCH_2SCH_2SCH_2)]$ (X = Cl, Br, or I)

	X in the complex		
	Cl	Br	I
θ_c/°C	−16.4	−25.8	−32.9
T_2^* [a]/s	0.15	0.208	0.183
Chemical shifts (Hz) [b]			
ν_A	585.0	609.4	649.9
ν_B	448.0	457.0	465.6
ν_C	439.0	441.7	442.3
ν_D	439.0	440.7	442.3
ν_E	407.0	409.9	414.3
ν_F	407.0	409.9	414.3
Coupling constants (Hz)			
$J_{AB} = J_{CD} = J_{EF}$ [c]	−15.0	−14.9	−15.1
$^3J(^{195}Pt-^1H_A)$	12.5	12.9	13.8
$^3J(^{195}Pt-^1H_B)$	1.0	0.0	1.0
$^3J(^{195}Pt-^1H_C)$	4.0	3.8	3.2
$^3J(^{195}Pt-^1H_D)$	4.0	3.8	3.2

[a] $T_2^* = (\pi\Delta\nu_{\frac{1}{2}})^{-1}$ where $\Delta\nu_{\frac{1}{2}}$ is the measured linewidth (Hz) at the half-height in the absence of exchange. [b] Relative to $SiMe_4$ using $CDCl_3$ as solvent. [c] Geminal coupling constants.

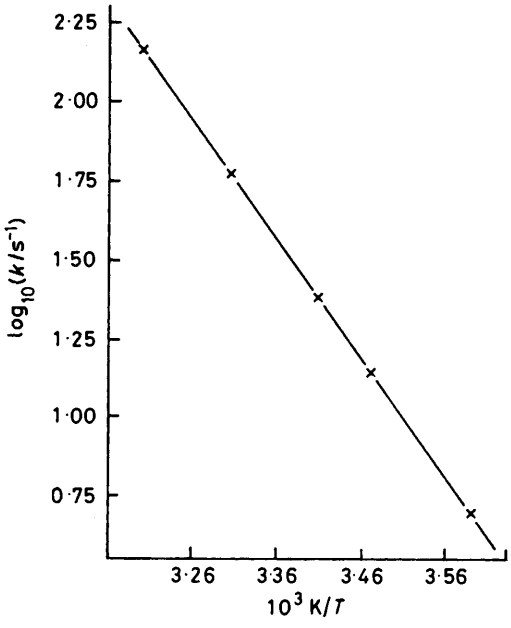

Figure 5. Arrhenius plot for the metal-pivoting rearrangement in $[(PtBrMe_3)_2(SCH_2SCH_2SCH_2SCH_2)]$

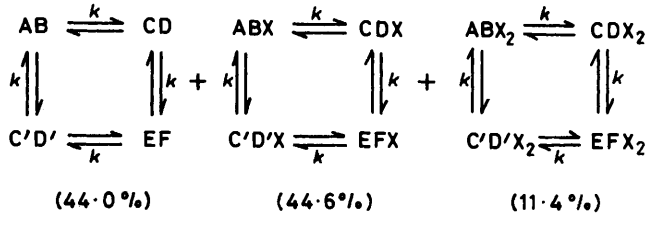

Scheme 1.

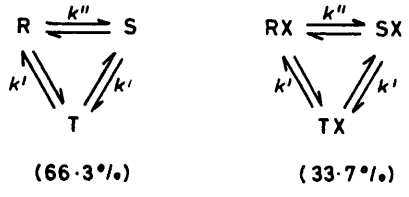

Scheme 2.

was varied independently of k', the rate constant for the interchange of equatorial and axial methyls by some type of scrambling process (see below).

Simulated and experimental spectra for the methyl-scrambling process in the bromo-complex are shown in Figure 6. Static ^1H n.m.r. spectral parameters used in the computations are given in Table 4.

Discussion

Static Hydrogen-1 N.M.R. Parameters.—The trends in the magnitudes of the parameters of the equatorial and axial Pt–Me groups are exactly analogous to those previously observed in other dinuclear Pt^{IV} complexes containing organosulphur ligands.[23,24,32]

Fluxional Rearrangements.—Metal-pivot intramolecular rearrangement. As stated earlier, lineshape changes in the ligand-methylene region of the ^1H n.m.r. spectra of the complexes $[(PtXMe_3)_2(SCH_2SCH_2SCH_2SCH_2)]$ are consistent with the occurrence of a metal-pivot motion similar to that previously observed in the corresponding complexes of trithiane. However, in contrast to the latter complexes, it is evident from the structure of the complexes under discussion that there is more than one conceivable rearrangement mechanism.

In Figure 8, mechanism (A) closely allies that for pivots in the trithiane complexes in that it proceeds *via* a seven-co-ordinate *transition state*. It differs in that it comprises a 90° 1,5-pivot as opposed to a 60° 1,3-pivot. Mechanism (B) entails the formation of an *intermediary* 1,5-co-ordinated species. In direct contrast to (A), the pivot can then proceed in a 1,3-fashion about either co-ordinated sulphur atom. Thus (B) ultimately results in one or both Pt atoms changing their co-ordination sites by two sequential 45° 1,3-metal pivots.

From a purely structural viewpoint, mechanism (A) is preferable. As a prerequisite to the occurrence of a pivot, a lone pair of electrons on an unco-ordinated S atom must be directionally orientated towards the commuting atom in such a way as to facilitate the rearrangement. Thus, if the ligand solely adopts a chair–boat conformation, as revealed by *X*-ray diffraction, it can be seen in Figure 9(*a*) that no such alignment exists. Frank *et al.*,[5] however, have reported the C–S backbone of tetrathiocane to have great flexibility. Thus, in solution other conformations, which are albeit less energetically favourable, should theoretically exist.

Figure 9(*b*) illustrates one such alternative structure in which the ligand moiety has a twisted chair-boat conformation, readily accessible from the above ground-state structure. It is apparent that a lone pair of electrons on S(4) is directed towards Pt(2). Very little further distortion of the ligand ring is necessary in order to manoeuvre these two atoms into a position whereby Pt(2) can possibly be co-ordinated to by both S(2) and S(4). This amounts to the formation of a seven-

Table 6. Arrhenius and Eyring activation parameters for metal pivoting (m.p.) and methyl scrambling (m.s.) in the complexes $[(PtXMe_3)_2(SCH_2SCH_2SCH_2SCH_2)]$

X	Process	$\log_{10} A$	E_a/kJ mol^{-1}	$\Delta H^{\ddagger}$/kJ mol^{-1}	$\Delta S^{\ddagger}$/J K mol^{-1}	$\Delta G^{\ddagger}$ (298.15 K)/kJ mol^{-1}
Cl	m.p.	14.44 ± 0.32	75.58 ± 1.82	73.13 ± 1.83	23.30 ± 6.19	66.15 ± 0.01
	m.s.	13.61 ± 0.15	70.50 ± 0.89	68.00 ± 0.88	7.33 ± 2.94	65.82 ± 0.01
Br	m.p.	14.13 ± 0.21	71.57 ± 1.19	69.16 ± 1.19	17.48 ± 4.10	63.95 ± 0.27
	m.s.	14.15 ± 0.11	71.67 ± 0.64	69.22 ± 0.64	17.81 ± 2.19	63.90 ± 0.01
I	m.p.	14.04 ± 0.53	67.66 ± 2.81	65.33 ± 2.80	16.05 ± 10.04	60.55 ± 0.19
	m.s.	14.27 ± 0.07	68.22 ± 0.36	65.95 ± 0.32	20.65 ± 1.20	59.79 ± 0.03

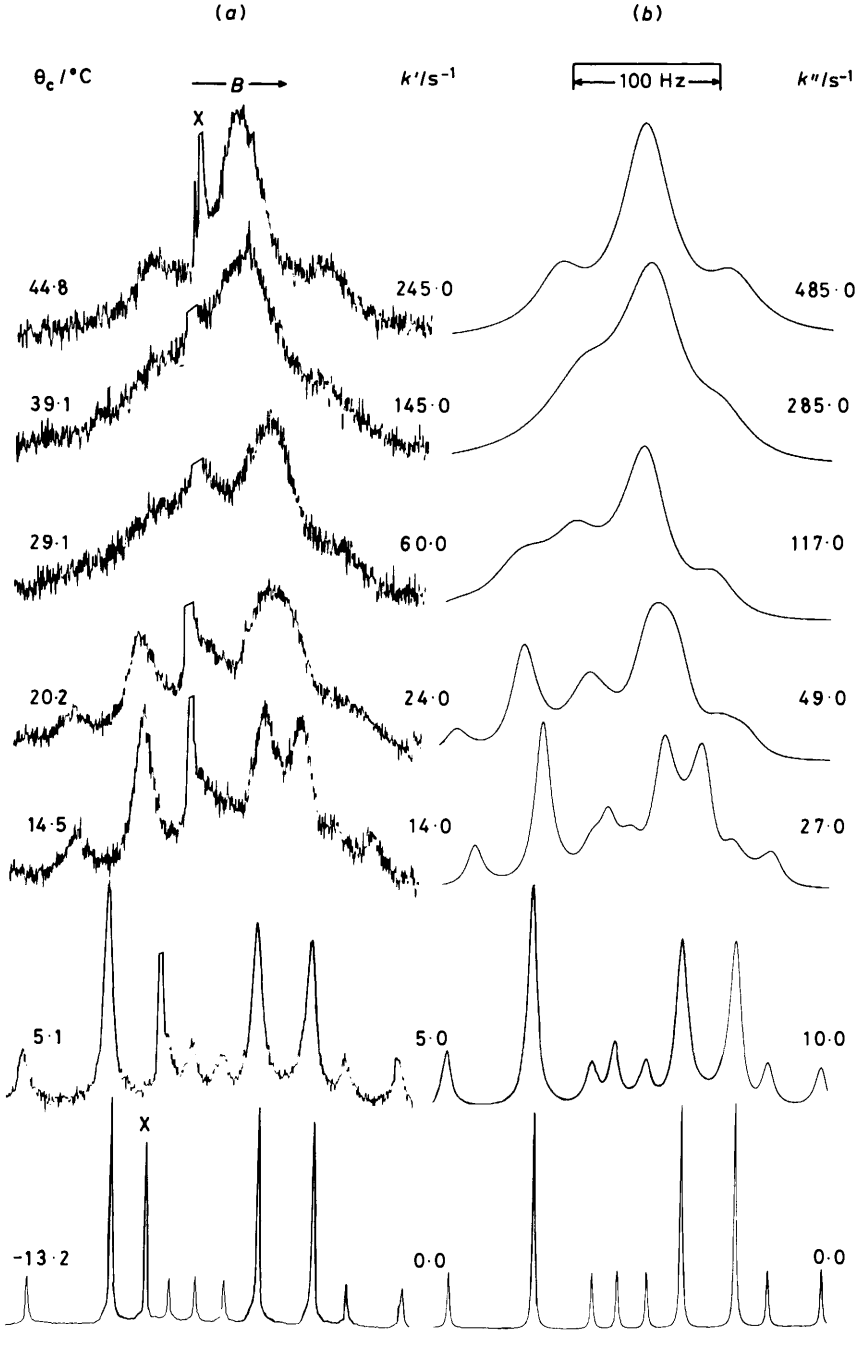

Figure 6. (*a*) Experimental and (*b*) computer-simulated spectra (Pt–methyl region) of $[(PtBrMe_3)_2(SCH_2SCH_2SCH_2SCH_2)]$, demonstrating the effects of intramolecular Pt–methyl scrambling (X = H_2O impurity)

co-ordinate transition state necessary for a metal pivot *via* mechanism (A).

Figure 9(*c*) represents the sole conformation by means of which a 1,5-intermediate species can be reached. Such a 'crown' orientation of the ligand would be far less energetically stable than that discussed above since electronic repulsion would be experienced between the lone pairs of S^3, S^4, and those of the bridging halogen atoms. Furthermore, a close examination of the molecular structure of a 1,5-intermediate (Figure 10) suggests that such a species is highly unlikely since severe electron repulsion would exist between the uncoordinated S atom lone pairs and those of the bridging halogen atoms.

Unequivocal support for the metal-pivot rearrangement proceeding *via* mechanism (A) was obtained by the following analysis of the methylene bandshape changes.

The interconversion of the eight possible permutation isomers of the complexes $[(PtXMe_3)_2(SCH_2SCH_2SCH_2SCH_2)]$ (X = Cl, Br, or I) by mechanisms (A) and (B) is represented diagrammatically in Figure 11. The associated dynamic nuclear magnetic spin problem is shown in Figure 12. The latter, as a consequence of the interrelation of different sets of isomers, is not identical for the two mechanisms. In mechanism (A), neither of the two platinum atoms is able to commute over all the S atoms. Thus, following the numbering scheme in Figure 9, Pt^1 is restricted to S^1 and S^3, and Pt^2 to S^2 and S^4. Thus, mechanism (A) will cause interconversion *within* the two sets of four isomers which are disposed on the two opposing faces of the cube (Figures 11 and 12), but no interconversion *between* the sets. Such a dynamic spin problem is represented by Scheme 1. In mechanism (B), each platinum atom can traverse over *all* the S atoms but with different weighted probabilities. A study of Figures 11 and 12 reveals that the spin problem may now be described according to Scheme 3.

Simulation of the experimental spectra of each complex was carried out employing, in turn, both these spin problems. Perfect pre-ligand-dissociation 'fits' were obtained only when Scheme 1 was used (see Figure 4).

Therefore, in the light of the above evidence, it is concluded that the coalescence phenomena observed to occur among the ligand methylene ^1H n.m.r. spectral resonances of the complexes $[(PtXMe_3)_2(SCH_2SCH_2SCH_2SCH_2)]$ (X = Cl, Br, or I) are a consequence of the dinuclear Pt^{IV} moiety undergoing a

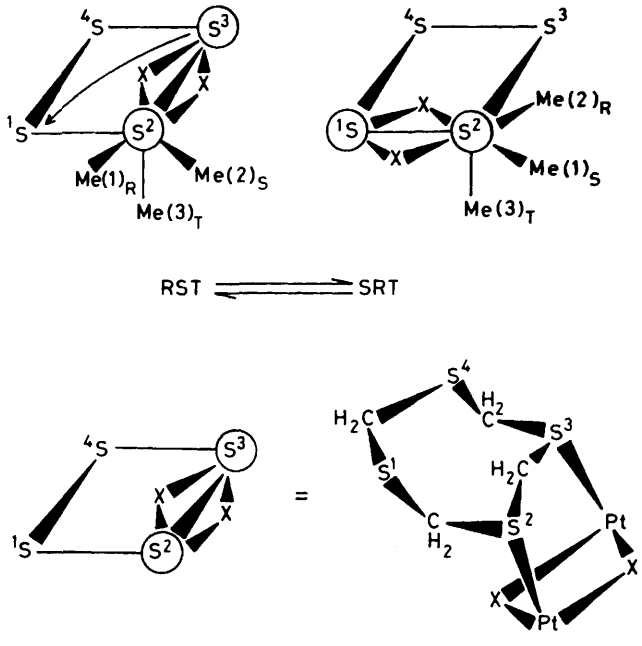

Figure 7. Effect of metal pivoting on the equatorial methyl groups attached to the pseudo-stationary Pt atom

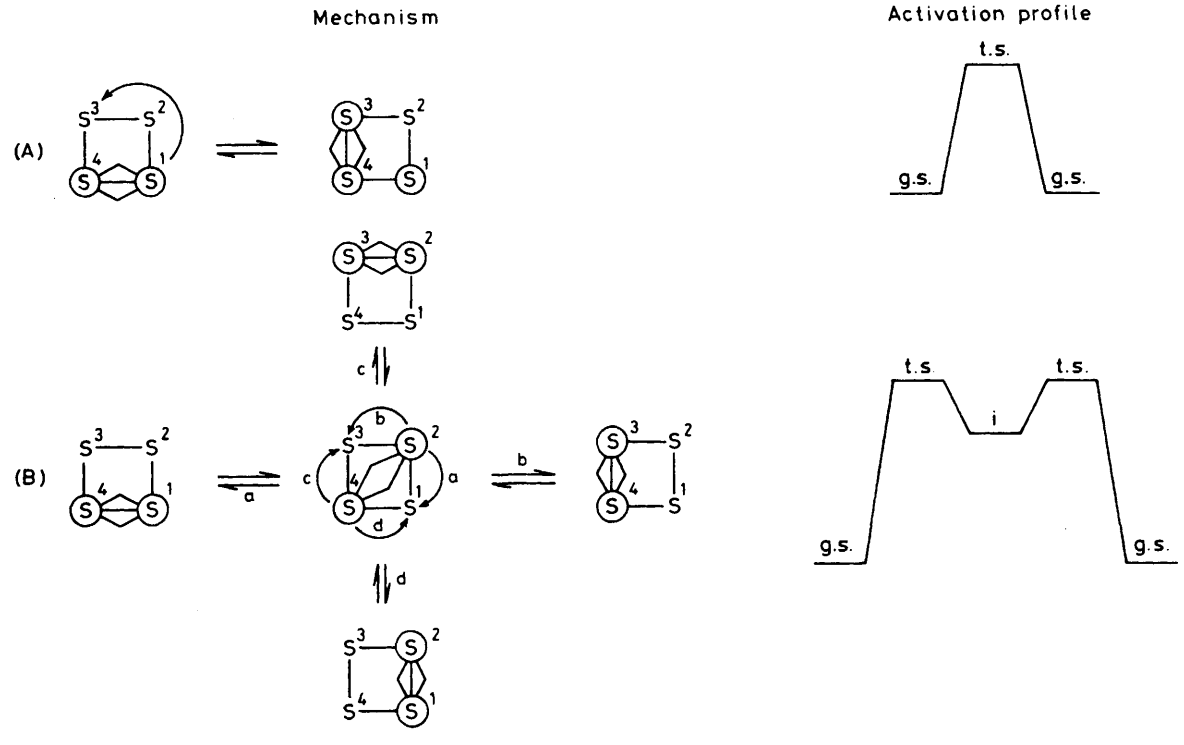

Figure 8. Alternative mechanisms for metal pivoting in dinuclear platinum(IV) complexes of 1,3,5,7-tetrathiocane: g.s. = ground state, t.s. = transition state, i = intermediate

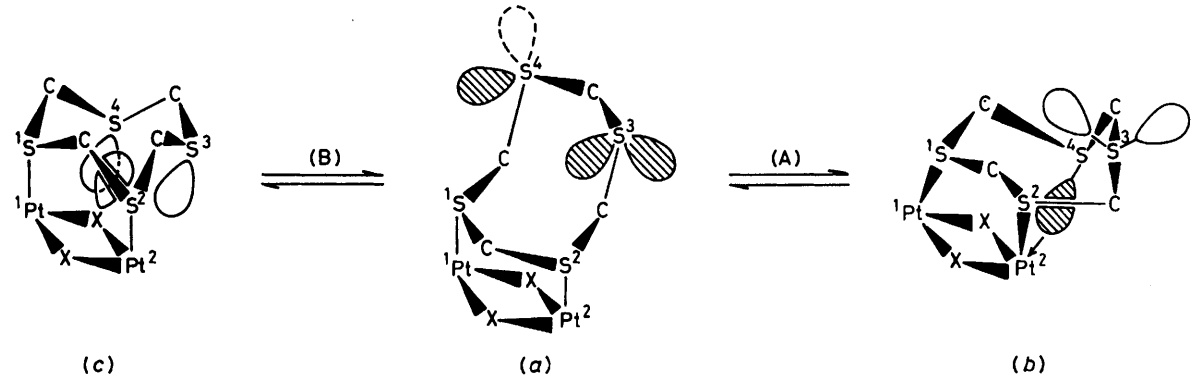

Figure 9. Postulated ligand conformational changes that occur during metal pivots by mechanisms (A) and (B) (see Figure 8)

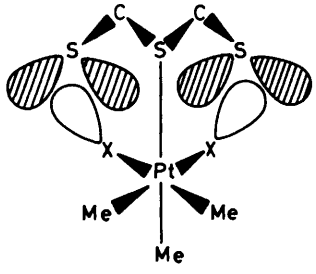

Figure 10. A possible structure for the 1,5-intermediate complex as viewed along the Pt · · · Pt axis

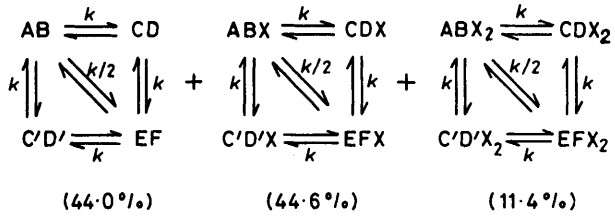

Scheme 3.

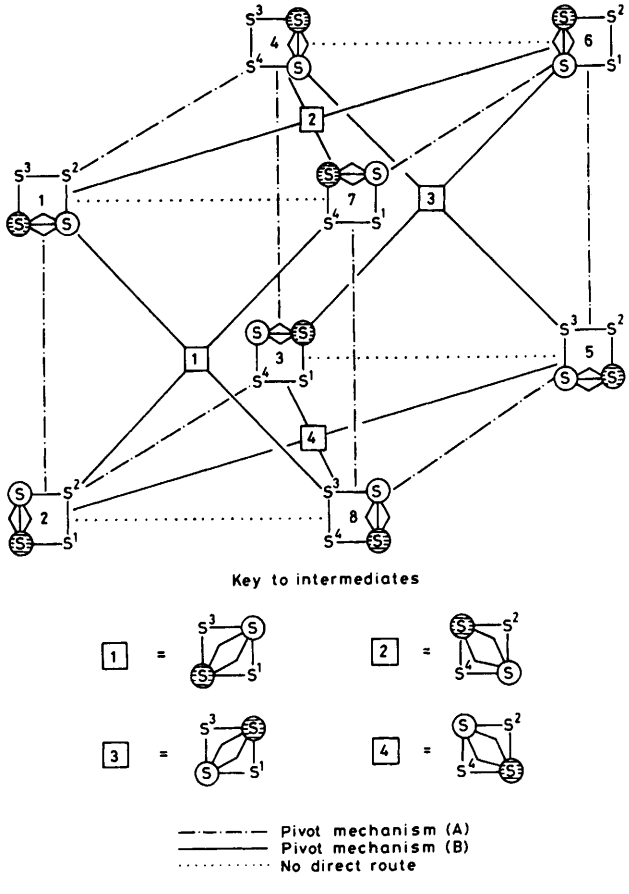

Figure 11. A representation of the eight permutation isomers of the complexes $[(PtXMe_3)_2(SCH_2SCH_2SCH_2SCH_2)]$ and their interrelation by the two alternative metal-pivot mechanisms

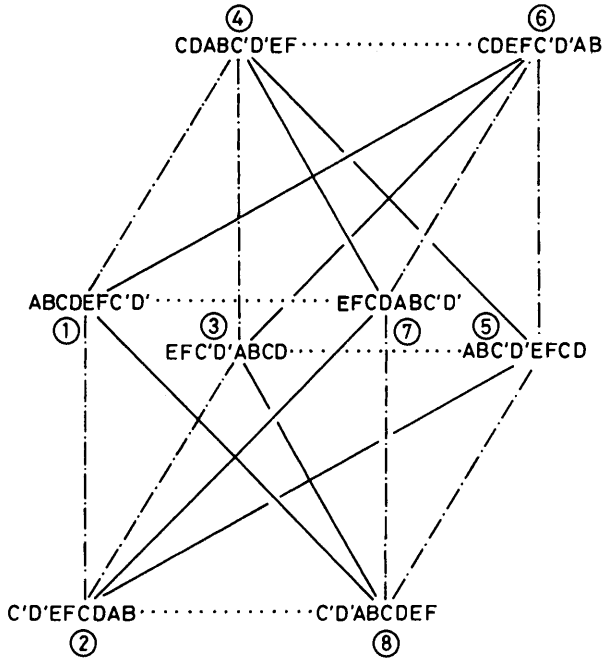

Figure 12. Full dynamic spin problem associated with Figure 11

series of 90° 1,5-metal pivots *via* a seven-co-ordinate transition state.

The straight-line Arrhenius plots (see Figure 5) corroborate the occurrence of a single fluxional process. The pre-exponential factor, $\log_{10} A$ (Table 6), for the pivot process in each of the complexes has a value in the range 13.5—14.5. This, in addition to a non-exchanging free-ligand peak in the n.m.r. spectra, is indicative of the intramolecularity of the process.

A comparison of the $\Delta G^{\ddagger}$ values for the pivot process in the tetrathiocane complexes (Table 6) with those for the trithiane complexes, the latter being 58.6 and 58.8 kJ mol^{-1} for X = Cl

Table 7. Energy parameters for methyl scrambling and other high-energy fluxional rearrangements in $[(PtXMe_3)_2L]$ complexes

L	X	Process [a]	$\log_{10} A$	$\Delta G^{\ddagger}$ (298.15 K)/kJ mol^{-1}	Ref.
MeSSMe	Cl	l.s.	12.8 ± 0.7	61.3 ± 0.4	
		m.s.	13.8 ± 0.4	62.4 ± 0.2	23
MeSeSeMe	Cl	l.s.	13.8 ± 3.8	65.1 ± 0.1	
		m.s.	13.8 ± 0.4	65.2 ± 0.1	23
MeSeSeMe	Br	l.s.	14.0 ± 0.5	64.5 ± 0.1	
		m.s.	13.2 ± 0.4	64.5 ± 2.2	23
MeSCH(Me)SMe	Cl	l.s.	13.1 ± 0.4	71.5 ± 0.2	
		m.s.	12.7 ± 0.6	71.6 ± 0.4	31
MeSeCH(Me)SeMe	Cl	l.s.	12.5 ± 1.2	72.6 ± 0.8	
		m.s.	12.6 ± 0.5	72.8 ± 0.4	31
$MeSCH_2SeMe$	Cl	l.s.	11.3 ± 0.1	69.5 ± 0.1	
		m.s.	14.6 ± 0.1	70.3 ± 0.1	32
$MeSCH_2SeMe$	Br	l.s.	13.3 ± 0.1	68.8 ± 0.1	
		m.s.	13.8 ± 0.1	67.6 ± 0.1	32
$MeSCH_2SeMe$	I	l.s.	11.5 ± 0.2	65.6 ± 0.1	
		m.s.	13.7 ± 0.1	64.8 ± 0.1	32
$HC(SMe)_3$	Cl	m.p.	13.9 ± 0.5	71.7 ± 0.2	
		m.s.	13.5 ± 0.1	71.9 ± 0.1	*b*
$HC(SMe)_3$	Br	m.p.	14.1 ± 0.4	69.5 ± 0.1	
		m.s.	14.1 ± 0.3	69.4 ± 0.1	*b*

[a] Abbreviations: l.s. = ligand switching, m.s. = methyl scrambling, m.p. = metal pivoting. [b] T. E. Mackenzie, University of Exeter, unpublished work.

and Br respectively,[2] reveals two interesting facts. Primarily, the values for the former are some 5 kJ mol^{-1} greater. In line with previous arguments, this could be a result of an increased skeletal flexibility of the ligand moiety, thus, reducing the availability of unco-ordinated chalcogen lone pairs.[4] This, however is unlikely to be the only contributing factor. The transition-state structure for the pivot process in the tetrathiocane complexes is more likely to have a relatively higher energy than that for the complexes containing trithiane, due to the greater distance and angle between the sulphur atom pair over which a Pt atom must commute. This, to a certain extent, is sustained by the $\Delta S^{\ddagger}$ values which are larger for the former, implying the transient species possesses more vibrational and rotational degrees of freedom.[33] Since the ground-state structures of both series of complexes are extremely similar this might well explain the observed halogen dependence of $\Delta G^{\ddagger}$ (decreasing in the order Cl > Br > I) for metal pivots in the tetrathiocane complexes, such a transition-state structure being more liable to be energetically affected by changes in its molecular constitution.

Increased ligand flexibility also appears to determine the relative ease of metal–ligand shifts in complexes of $[M(CO)_5]$. The tetrathiocane ligand has recently [34] been used to form complexes with $[Cr(CO)_5]$ and $[W(CO)_5]$. Fluxional metal shifts have been observed, although it is not certain whether these movements are 1,3- or 1,5-shifts. Irrespective of their mechanism, a comparison with the trithiane complex analogues [4] shows an increase of *ca.* 5 kJ mol^{-1} in the $\Delta G^{\ddagger}$ values for the tetrathiocane complexes.

Platinum–methyl scrambling. The activation parameters for this process, using the spin problem denoted in Scheme 2, are listed in Table 6. A close examination reveals that the data of the methyl-scrambling and ligand-pivoting motions are equal within experimental error. In other platinum(IV) complexes where ligand 180° switching and platinum–methyl scrambling processes occur,[32] similar near-equalities of barrier energies were noted. This has led to the proposal [32] that the ligand fluxion and the methyl scrambling are different manifestations of a single fluxional transition state rather than being independent rearrangements. The same situation appears to apply here in the case of ligand pivoting and Pt–methyl scrambling. Further insight into this problem was gained in the present work from the observation that the rate of exchange between the two equatorial Pt methyls (k'' in Scheme 2) was consistently a factor of two greater than that between equatorial and axial Pt methyls (k' in Scheme 2) as exemplified in Figure 5. Furthermore, the methyl-exchange rate constant k' was equal to that of the ligand pivot process (k in Scheme 1 and Figure 4) at any chosen temperature. These observations afford evidence that the two processes have the same activation energy and a common transition state. We now describe a possible mechanism whereby this could be achieved.

From the full dynamic spin problem (Figure 12) it is clear that, for a 90° 1,5-metal pivot [Figure 8, mechanism (A)] from any spin isomer, equation (1) applies, where '+ pivot' and

$$k(\text{total pivot}) = k(+\text{ pivot}) + k(-\text{ pivot}) \quad (1)$$

'− pivot' represent clockwise and anticlockwise pivots respectively.

For a complete cycle of four clockwise pivots it is clear (Figure 12) that the methylene protons, AB, exchange for 50% of the manoeuvres with CD and 50% with C′D′: thus equations (2) and (3) apply. Similar relationships can be

$$k(\text{AB}\rightarrow\text{CD}) = \tfrac{1}{2}k(+\text{pivot}) \quad (2)$$

$$k(\text{AB}\rightarrow\text{C'D'}) = \tfrac{1}{2}k(-\text{pivot}) \quad (3)$$

obtained for anticlockwise pivots. Since $k(+\text{pivot}) = k(-\text{pivot})$, this gives equation (4).

$$k(\text{total pivot}) = 2k(+\text{pivot}) = 4k(\text{AB}\rightarrow\text{CD}) \quad (4)$$

We have shown earlier that a 1,5-metal pivot necessarily causes an interchange only of the two equatorial Pt–methyl groups on the pseudo-stationary platinum atom (Figure 7). However, axial–equatorial methyl averaging is also clearly evident from the spectra.

We now postulate that this averaging can be explained in terms of ±120° rotations of the $PtMe_3$ moiety about its three-fold rotation cone axis. Such an averaging can occur only on

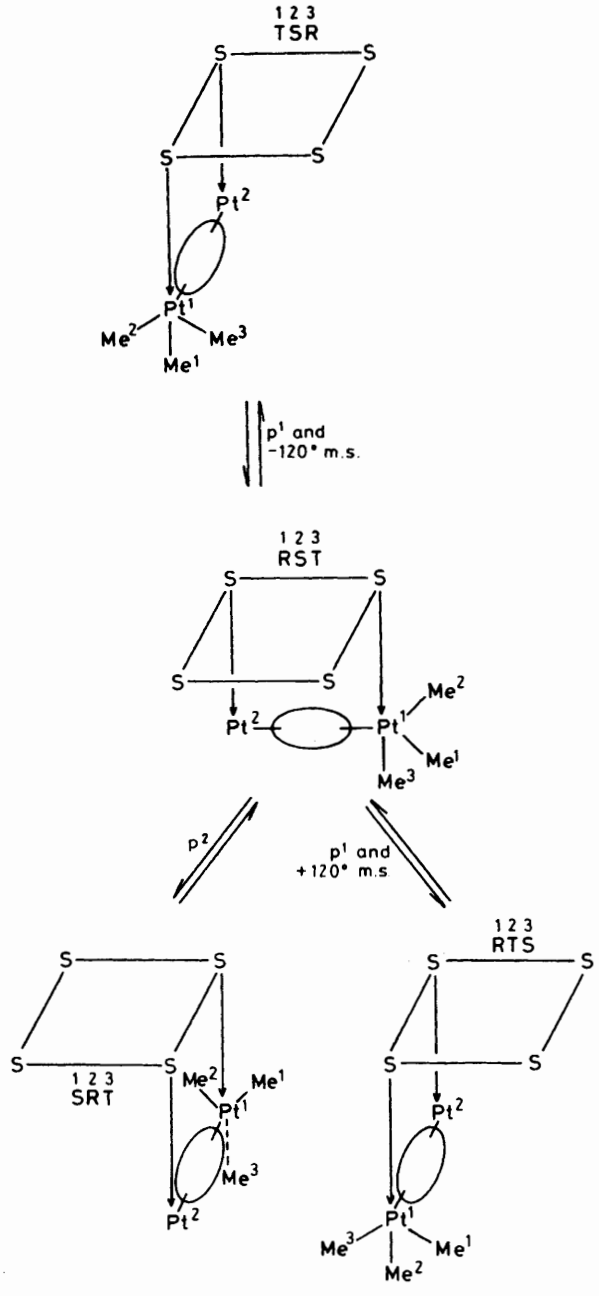

Figure 13. Interconversion of the Pt–methyl environments as a result of incidental averaging on the pseudo-stationary Pt atom and 120° rotations of the pivot-commuting $PtMe_3$ moiety: p^1 = 1,5-pivot of Pt^1, p^2 = 1,5-pivot of Pt^2

the pivot-commuting Pt atom of the dinuclear unit, and results in two additional methyl-group permutation isomers (Figure 13). Axial–equatorial averaging thus occurs on the pivot commuting Pt and equatorial–equatorial averaging on the pseudo-stationary Pt. In general, there are six permutation isomers of the $PtMe_3$ groups. These are depicted in Figure 14 where it follows that the total rate of interconversion of isomers can be expressed as in equation (5), where k(i.e.) is the rate

$$k'(\text{total}) = k(\text{i.e.}) + k(+120°) + k(-120°) \quad (5)$$

constant for the incidental averaging of the equatorial environments due to the pivot process, and $k(+120°)$ and $k(-120°)$ are the rate constants for the clockwise and anti-

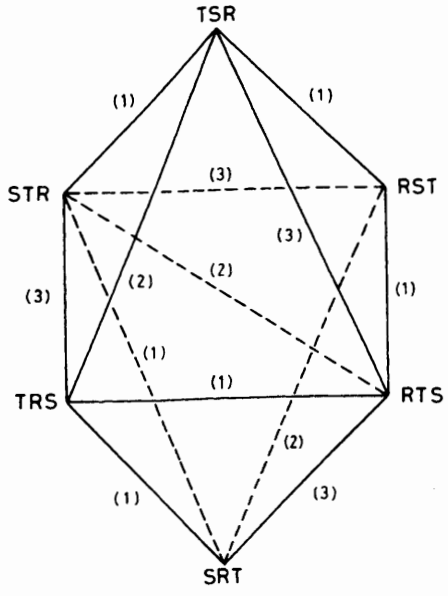

Figure 14. A representation of the six permutation isomers of the $PtMe_3$ group and their interrelations as a result of metal pivoting and $PtMe_3$ group rotations: (1) exchange on pivot-commuting Pt, (2) incidental exchange on pseudo-stationary Pt, (3) no direct exchange

clockwise rotations of the $PtMe_3$ moiety on the commuting Pt atom.

If $PtMe_3$ rotations occur concurrently with 1,5-pivots, then equation (6) applies and since clockwise and anticlockwise rotations are equally likely this leads to equation (7). Equations (8) and (9), where RS refer to the two equatorial Pt methyls, follow from equation (5).

$$k(\text{i.e.}) = k(+120°) + k(-120°) \quad (6)$$

$$k(\text{i.e.}) = 2k(+120°) \quad (7)$$

$$k'(\text{total}) = 2k(\text{i.e.}) \quad (8)$$

$$= 2k(\text{RS}) \quad (9)$$

From equations (1) and (14) (see below) it is clear that we can write equation (10) which gives directly equation (11), or, using the nomenclature of Schemes 1 and 2, equation (12). Thus, the rate of equatorial–equatorial Pt–methyl averaging is twice that of methylene exchanges. Now, by combining equations (7)—(11), equation (13) follows, and since one 120° rotation has the effect of exchanging an axial and equatorial en-

$$k'(\text{total}) = k(\text{total pivot}) \quad (10)$$

$$2k(\text{AB}\rightarrow\text{CD}) = k(\text{RS}) \quad (11)$$

$$2k = k'' \quad (12)$$

$$k(\text{AB}\rightarrow\text{CD}) = k(+120°) \quad (13)$$

$$k(+120°) = k' \text{ (Scheme 2)} \quad (14)$$

vironment, then this gives equation (14). Thus $k = k'$; and in summary, $k'' = 2k = 2k'$.

These results are in direct agreement with the observed relationships of the 'best fit' rate constants for the Pt–methyl region (Figure 6) and the ligand-methylene region (Figure 4) spectra. They confirm that Pt–methyl exchanges can be

explained in terms of a combination of incidental exchanges of equatorial methyls on the pseudo-stationary Pt and axial–equatorial methyl exchanges on the pivot-commuting Pt atom. This interpretation has the advantage over pseudo-random Pt–methyl scrambling mechanisms [*e.g.* rhombic (Ray-Dutt) or trigonal (Bailar) twists] [35] in that only a single reorientation axis is postulated. In such random scrambling processes, the pseudo-rotation axes through either six-co-ordinate Pt atom must all be taken as equivalent, and re-orientation must take place about any of these axes with equal probability. This assumption is not easily justified, although it appears to hold in trigonal-bipyramidal systems with symmetries lower than the regular D_{3h}.[36]

It should, however, be mentioned that a random methyl-scrambling process in conjunction with a 1,5-metal pivot process would equally well explain the present dynamic n.m.r. observations. In this case, the Pt–methyls R, S, and T would each interconvert with a rate constant k', whilst R and S would also interconvert as a result of the 1,5-pivot with a rate constant k. Since $k = k'$, then the rate of equatorial–equatorial averaging would again be twice that of axial–equatorial averaging.

Our present studies therefore do not permit a clear distinction between a non-random rotation process and a random bond-angle distortion process. However, for the reason mentioned earlier we favour the non-random process, and also because this mechanism ascribes the ligand pivoting and Pt–methyl rearrangements to a single transition state.

Previous studies of trimethylplatinum(IV) complexes have not provided such detailed insight into the mechanism of the scrambling process, either because the equatorial Pt methyls were already isochronous before the onset of methyl scrambling, or because their chemical shift differences were too small to cause their signals to be sensitive to the rate of exchange of their environments.[23,24,31,32,37,38]

Table 7 presents data of other trimethylplatinum(IV) complexes where methyl scrambling occurs concurrently with other high-energy fluxional rearrangements. This is further corroborative evidence for the two processes being separate manifestations of a single transition state rather than independent rearrangements.

Interestingly, methyl scrambling does not occur concurrently with 1,3-methyl pivots in the complexes $[(PtXMe_3)_2(SCH_2SCH_2SCH_2)]$ (X = Cl or Br).[2] Since the transition state differs from that of the tetrathiocane complexes, it would appear that for the trithiane complexes the transient species produced are neither structurally favourable nor sufficiently activated additionally to exchange the Pt–methyl environments.

For $[(PtXMe_3)_2(SCH_2SCH_2SCH_2SCH_2)]$, however, their dynamic n.m.r. behaviour can be rationalised in terms of 90° 1,5-metal pivots and 120° rotations of the pendant $PtMe_3$ moiety, both movements being resultants of a single seven-co-ordinate platinum(IV) transition state.

References

1 E. W. Abel, S. K. Bhargava, and K. G. Orrell, *Prog. Inorg. Chem.*, in the press.
2 E. W. Abel, M. Booth, G. D. King, K. G. Orrell, G. M. Pring, and V. Šik, *J. Chem. Soc., Dalton Trans.*, 1981, 1846.
3 E. W. Abel, M. Booth, K. G. Orrell, and G. M. Pring, *J. Chem. Soc., Dalton Trans.*, 1981, 1944.
4 E. W. Abel, G. D. King, K. G. Orrell, G. M. Pring, V. Šik, and T. S. Cameron, *Polyhedron*, 1983, **2**, 1117.
5 G. W. Frank, P. J. Degen, and F. A. L. Anet, *J. Am. Chem. Soc.*, 1972, **94**, 4792.
6 J. E. Anderson, *J. Chem. Soc. B*, 1971, 2030.
7 M. Schmidt, K. Blaettner, P. Kochendörfer, and H. Ruf, *Z. Naturforsch., Teil B*, 1966, **21**, 622.
8 M. Schmidt and E. Weissflog, *Z. Anorg. Allg. Chem.*, 1974, **406**, 271.
9 J. C. Baldwin and W. C. Kaska, *Inorg. Chem.*, 1975, **14**, 2020.
10 W. J. Pope and S. J. Peachey, *J. Chem. Soc.*, 1909, 571.
11 D. E. Clegg and J. R. Hall, *J. Organomet. Chem.*, 1970, **22**, 491.
12 E. W. Abel, A. K. Ahmed, G. W. Farrow, K. G. Orrell, and V. Šik, *J. Chem. Soc., Dalton Trans.*, 1977, 47.
13 D. A. Kleier and G. Binsch, DNMR3 Program 165, Quantum Chemistry Program Exchange, Indiana University, 1970.
14 G. Binsch and H. Kessler, *Angew. Chem., Int. Ed. Engl.*, 1980, **19**, 411.
15 S. Motherwell, PLUTO Crystal and Molecular Structure Plotting Program, Cambridge Crystallographic Centre, 1980.
16 R. E. Rundle and J. H. Sturdivant, *J. Am. Chem. Soc.*, 1947, **69**, 1561.
17 E. L. Burovoya, *Trudy Inst. Krist. Acad. Nauk. SSSR*, 1949, **5**, 197; *Chem. Abstr.*, 1953, **47**, 3749.
18 E. W. Abel, M. Booth, T. S. Cameron, K. G. Orrell, and G. M. Pring, *J. Chem. Soc., Chem. Commun.*, 1981, 29.
19 G. M. Pring, Ph.D. Thesis, University of Exeter, 1982.
20 C. D. Cowman, J. C. Thiebeault, R. F. Ziolo, and H. B. Gray, *J. Am. Chem. Soc.*, 1976, **98**, 3209.
21 M. P. Brown, R. J. Puddephatt, M. Rashidi, Lj. Manojlovic-Muir, K. W. Muir, T. Solomon, and K. R. Seddon, *Inorg. Chim. Acta*, 1977, **23**, L33.
22 G. W. Frank and P. J. Degen, *Acta Crystallogr., Sect. B*, 1973, **29**, 1815.
23 E. W. Abel, A. R. Khan, K. Kite, K. G. Orrell, and V. Šik, *J. Chem. Soc., Dalton Trans.*, 1980, 2220.
24 E. W. Abel, A. R. Khan, K. Kite, K. G. Orrell, and V. Šik, *J. Chem. Soc., Dalton Trans.*, 1980, 1169, 1175.
25 D. E. Clegg, J. R. Hall, and G. Swile, *J. Organomet. Chem.*, 1972, **38**, 403.
26 E. Campaigne, N. F. Chamberlain, and B. E. Edward, *J. Organomet. Chem.*, 1962, **27**, 135.
27 P. L. Goggin, R. J. Goodfellow, and F. J. S. Reid, *J. Chem. Soc. A*, 1971, 2031.
28 M. P. Brown, R. J. Puddephatt, M. Rashidi, and K. R. Seddon, *J. Chem. Soc., Dalton Trans.*, 1978, 516.
29 M. P. Brown, J. R. Fischer, S. J. Franklin, R. J. Puddephatt, and K. R. Seddon, *J. Chem. Soc., Chem. Commun.*, 1978, 749.
30 M. Karplus, *J. Chem. Phys.*, 1959, **30**, 11; *J. Am. Chem. Soc.*, 1963, **85**, 2870.
31 E. W. Abel, A. R. Khan, K. G. Orrell, and V. Šik, *J. Chem. Soc., Dalton Trans.*, 1980, 2208.
32 E. W. Abel, K. G. Orrell, V. Šik, and B. L. Williams, *J. Chem. Soc., Dalton Trans.*, 1981, 2439.
33 A. A. Frost and R. G. Pearson, 'Kinetics and Mechanism,' 2nd edn., Wiley, New York, 1961.
34 E. W. Abel, G. D. King, K. G. Orrell, and V. Šik, *Polyhedron*, 1983, **2**, 1363.
35 F. A. Cotton and G. Wilkinson, 'Advanced Inorganic Chemistry,' 4th edn., Wiley, New York, 1980, pp. 1223—1225.
36 K. Mislow, *Acc. Chem. Res.*, 1970, **3**, 321.
37 E. W. Abel, S. K. Bhargava, K. Kite, K. G. Orrell, V. Šik, and B. L. Williams, *J. Chem. Soc., Dalton Trans.*, 1982, 583.
38 E. W. Abel, M. Z. A. Chowdhury, K. G. Orrell, and V. Šik, *J. Organomet. Chem.*, 1983, **258**, 109.

Received 13*th December* 1983; *Paper* 3/2197